Proceedings Paper:
Meng, W, Sheng, B, Klinger, M et al. (2015) Design and control of a robotic wrist orthosis for joint rehabilitation. In: Advanced Intelligent Mechatronics (AIM), 2015 IEEE International Conference on. IEEE ASME International Conference on Advanced Intelligent Mechatronics, 07-11 Jul 2015, Busan, South Korea. IEEE/ASME, pp. 1235-1240. ISBN: 1467391077.

Design and Control of a Robotic Wrist Orthosis for Joint Rehabilitation*

Wei Meng, Bo Sheng, Michael Klinger, Quan Liu, Zude Zhou, Sheng Q. Xie*, *Senior Member, IEEE*

***Abstract*—Ageing society in many countries has led to an increasing number of stroke and cerebral palsy patients who require rehabilitation therapy. Affected wrist joints often show an increased spasticity and stiffness, caused by impairments of surrounding muscles and tendons. However, the medical devices for wrist joint assessment and rehabilitation are lacking. This paper proposes a robotic orthosis to assist the patient's wrist to perform rehabilitation exercise in a compliant way. A 1-DOF robotic device with parallel mechanism is designed for the wrist joint by utilising pneumatic artificial muscles (PAMs) that are compliant and lightweight. The mechanical design of the wrist orthosis and the corresponding development of pneumatic control system will be also presented. A model-based pressure close-loop control strategy is implemented for the PAMs in order to track the trajectory in high-performance. Experiments on the orthosis demonstrated that the robot could assist the hand to move along a torque-sensitive trajectory with relatively small errors and the differential forces were also kept stable.**

***Keywords*—wrist orthosis; joint rehabilitation robot; pneumatic artificial muscles (PAMs); pressure control**

I. INTRODUCTION

Paralysis is a loss of muscle functionality that is usually caused by damage to the nervous system of the human body, rather than damage to the muscle itself. Common causes for paralysis are stroke, head injuries, spinal cord injuries, multiple sclerosis or cerebral palsy [1]. Being impaired or completely unable to perform motor and sensor tasks, paralysis is likely to have a huge impact on a patient's life [2]. Rehabilitation is inevitable to maintain the flexibility of the locomotor system and to regain the motor abilities. The method of rehabilitation needs to be adapted to patient's capability to move, depending on the extent of initial injury. In this context, "active" exercises involve patient in moving a limb on his own, while "passive" exercises require the support of a therapist, who moves the limb manually [3]. The lack of motion in a joint can lead to the contracture of the attached muscles, thereby increasing the stiffness of the joint and reducing its range of motion [4].

The number of patients with paralysis is expected to grow over the next years, since most of the industrial countries are facing demographic changes towards an ageing society. This is due to the fact that the triggering deceases, first and foremost stroke is most common among older people. While 22% of people experiencing stroke die in the first 30 days, almost 80% of the survivors require the rehabilitation therapy [5]. Since manual therapy is extremely labour intensive and therefore cost much, industry has started to seek solutions for this problem. The rehabilitation robotics has thus seen continuous growth over the last years. Huge efforts have been expended in the field of soft robotics, in order to make robotic solutions safer while interacting with humans. This involves not only the development of novel soft actuators, but also the utilization of sensor systems for force or environmental monitoring in order to alleviate collisions or overusing joints [6].

Using robots for rehabilitation purposes offers several advantages [7]. Human therapists tend to fatigue during the exercises, thus being limited in the number of patients to treat. Highly accurate force and torque measurements allow robots to provide active movement support for a maximum training effect during the therapy. Furthermore, rehabilitation devices can be coupled with virtual reality, which increases fun and motivation for patients [8]. Recent studies [9] have shown that patient participation is a key feature for rehabilitation. Finally, these systems allow recording of information about patient's performance for eventual analysis and comparison [10].

However, many existing wrist robotic devices are driven by rigid actuators which are uncompliant, cumbersome, and unwearable [11]. Recently, an increasingly employed actuator in rehabilitation robotics is the soft (McKibben) pneumatic artificial muscle (PAM), working based on the principle of human muscle [12, 13]. Consisting of a tube-like bladder, surrounded by a braided mesh shell, the muscle contracts when pressurised and thereby induces an axial force. The actuator has an outstanding power-to-weight-ratio, natural compliance as well as pneumatic related advantages, such as compactness, cleanliness and simplicity [14]. Recent progress in pneumatic components, such as high speed solenoid and servo valves, as well as novel control strategies have brought about an increasing dissemination of the muscles [15, 16]. However, few current work has presented the applications of PAMs in wrist robots. Moreover, control of these actuators proves to be difficult, due to their highly non-linear behaviour.

Purpose of this paper is to describe the design and control of a wrist orthosis device for the joint rehabilitation using two PAMs in an antagonistic setup. In this case, the flexion and extension of the wrist joint are examined with the help of a 1-DOF device. In the following section, the mechanical design is illustrated. Afterwards, the control strategy is explained in details, and the results are presented.

*Resrach supported by National Natural Science Foundation of China (Grant No. 51475342) and Chinese Scholarship Council (CSC).

W. Meng, B. Sheng, M. Klinger and S. Q. Xie are with the Department of Mechanical Engineering, University of Auckland, Auckland 1142, New Zealand (correspondence author: S. Q. Xie, s.xie@auckland.ac.nz).

W. Meng, Q. Liu and Z. Zhou are with the School of Information Engineering, Wuhan University of Technology, Wuhan 430070, China. (e-mail: Wei Meng, wmen386@aucklanduni.ac.nz).

II. Device Design

In this section, the basic mechanical design of the wrist orthosis will be presented, and the force distribution over the pneumatic actuators will be explained.

A. Mechanical Design

The orthosis is designed to fit on the back of the patient's forearm, which is why the device weight is meant to be kept as low as possible. The PAMs used here are the Festo Fluidic Muscles DMSP20 [17] with an effective length of 90mm. The mechanical hinge is placed coaxial with the biological joint, which requires the connection of the muscles with the hinge pulleys through a redirected steel wire. Ball bearings are used to reduce friction in the hinge. Miniature in-line load cells are mounted on each muscle to measure the axial force. Figure 1 shows mechanical design of the wrist orthosis.

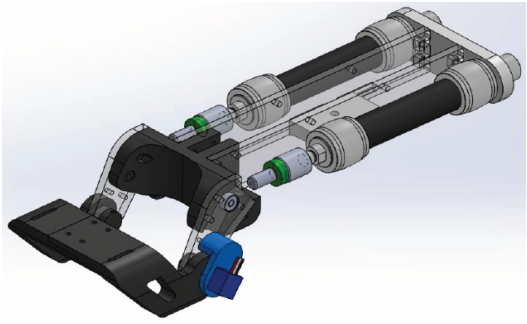

Figure 1. Mechanical design of the robotic wrist orthosis.

B. Force Distribution

Considering that both PAMs are fixed to the frame, the muscles, the wire-connections and the hinge pulleys create a closed system. For the force distribution model, both muscles need to be pressurised in initial position, so that the wire connections are under tension (with the muscle lengths still being equal: $l_1 = l_2$). This offset point is desirably found to be $l_{offset} = l_{max}/2$, in order to achieve the same contraction/ relaxation potential length in each direction. For any further movements, the muscle lengths should follow this rule:

$$l_1 + l_2 = 2 \cdot l_{offset} = const. \quad (1)$$

Assuming that the double hinge of the hand rest can be considered as a single constant radius pulley, the basic force distribution illustrated in Figure 2 is agreeable.

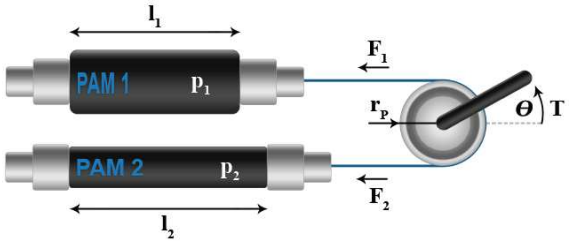

Figure 2. Force distribution in the orthosis.

To guarantee the hand rest's angular displacement, given the constant radius of the pulley r_p, θ can be expressed as:

$$\theta_{deg} = \frac{l_0 - l_1}{2 \cdot \pi \cdot r_p} \cdot 360 \cdot \quad (2)$$

As long as no torque T is applied, the forces F_1 and F_2 are equal. For an attached load, the distribution becomes:

$$F_1 + \frac{T}{r_p} - F_2 = 0 \cdot \quad (3)$$

which means the torque T can be explained by the differential force F_2-F_1, without the total force F_1+F_2 having any influence on the torque measurement. Consequently, any inaccuracies within the muscle's displacement control would not affect the torque control results.

C. Robotic Orthosis

Two Festo Fluidic Muscles are used as the antagonistic actuators and are placed on a plastic plate, which is strapped on the back of the patient's forearm. Both muscles are attached to a mechanical hinge through a steel wire. The wires are guided around the cylindrical hinge in a way, so that one PAM rotates it in a clockwise direction, and the other PAM in a counter clockwise direction when contracting. The hinge is located approximately 40mm above the biological wrist joint. A hand rest is connected to it to fix the hand during operation.

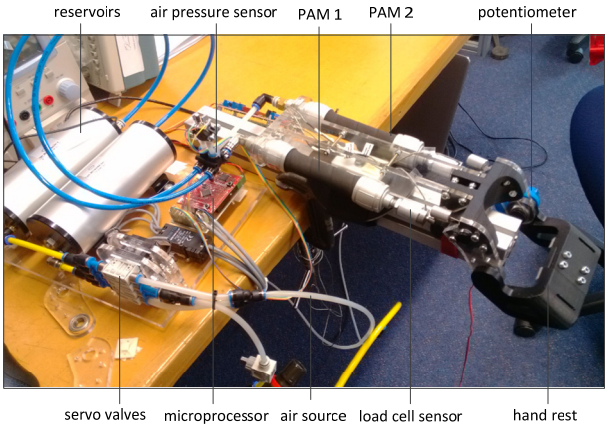

Figure 3. Setup of the robotic orthosis system.

A compact load cell is placed in-line with the wire-connection for each muscle. The mechanical hinge however is split into two metal pulleys, placed on each side of the wrist. Those are fixed to the hand rest and rotate within ball bearings in order to avoid friction. Furthermore, a potentiometer is utilised as an angle sensor, placed on the outside of the hinge's left pulley. The materials used in the device's frame are either 3D printed plastic or laser-cut acrylic resin, which leads to a low overall weight of 1086g. The hand rest located under the frame has an adjustable position, allowing it to customize the device for specific patient. Any other electrical and pneumatic components are placed on a remote board. Experiment setup of the robotic wrist orthosis is presented in Figure 3.

III. CONTROL STRATEGY

Recent papers have shown different approaches for controlling similar actuators, using either expensive servo valves or a pair of fast switching on/off valves. While utilising digital valves only, a proper control strategy needs to be implemented. Pulse width modulation has been proved to be superior to a bang-bang controller, thus being adopted here.

A. Pneumatic Setup

Figure 4 illustrates the pneumatic setup for one PAM. Two digital high speed valves Festo MHJ9 are utilized to control the air flow into and out of the muscle. With one being the inlet valve, allowing air to travel from the pressure source into the muscle, the second valve works as an exhaust, allowing to deflate the muscle. In order to set a specific pressure in the PAM, the opening times of both valves need to be controlled. The valves are operated via pulse width modulation, running at 50Hz. The magnitude and direction of the air flow is obtained by altering the pulse widths for both valves. The valves are energised through the supplied Festo MHJ9-KMH valve amplifier, which operates at 24V DC.

Given a small muscle volume (approx. 0:03l) and a high nominal flow rate of the valve (160l=min for a 6bar pressure gradient), the permanent air flow generates great vibration on the actuators. To solve this problem, an additional air reservoir is connected to the valves and the PAM to reduce this effect and stabilise the pressure. However, the increased volume may dampen the actuators step response. But it is not a major drawback, since fast movements are not required within the wrist training process. Furthermore, an air pressure sensor is equipped between the valves and the PAM to provide pressure feedback. Since the actual flow rate depends equally on the pressure gradient across the valve, the relation between the pulse width and the flow rate needs to be linearized.

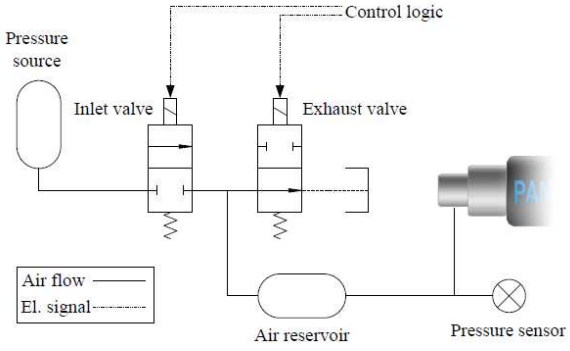

Figure 4. The pneumatic setup used for PAMs.

B. Actuator Linearization

Goal of the PWM principle is to control the air flow rate in a linear manner. However, it is not enough to adjust the timing of the two valves, since the air flow rate additionally depends on the pressure gradient across the valve's ports. This interdependency can be resolved to a linear behaviour with the help of compensation algorithms. Neglecting temperature effects, the flow rate Q through a valve is defined as:

$$Q = C_V \cdot \sqrt{\frac{\Delta p}{S_G}} \cdot \tag{4}$$

where C_V is the flow coefficient of the valve, and S_G the specific gravity of the gas. Both of these parameters are constant, thus being substituted to a_V . Given that the pressure gradient Δp and thus the flow rate Q becomes 0 when $pG = pS$ for the inlet, and $pG = 0$ for the exhaust, a linearization over the whole pressure range is not possible (pS is the supply pressure, pG is the gage pressure in the muscle). The pressure gradient Δp_i across the valve i differs for the inlet and the exhaust valve:

$$\Delta p_{inlet} = p_{source} - p_{muscle} \cdot \tag{5}$$

$$\Delta p_{exhaust} = p_{muscle} - 0 \cdot \tag{6}$$

The resulting air flow rate for each valve during PWM operation is a fractal of the nominal flow rate, depending on the adjusted duty cycle τ of the square-wave signal:

$$Q_i = \tau_i \cdot a_V \cdot \sqrt{p_i} \cdot \tag{7}$$

The total flow rate into/out of the muscle Q results in:

$$Q = a_V \cdot (\tau_{inlet} \cdot \sqrt{\Delta p_{inlet}} - \tau_{exhaust} \cdot \sqrt{\Delta p}_{exhaust}) \cdot \tag{8}$$

C. PAM Modelling

The relations between displacement, force and pressure of pneumatic actuators are highly non-linear. This behaviour, however, can be investigated in advance in order to look up or calculate the actuator parameters to be utilised later, based on measurement of other parameters [18]. In this case, it is always desired to obtain a certain displacement of the muscle, which can be achieved by controlling the pressure in it. The force induced by the muscle, is measured with the help of the load cell, allowing to be compensated for accurate displacement.

The generation of a model can be achieved in two different ways. A mathematical model can be created by establishing all relevant relations of the physical parameters involved in the system. This way is usually chosen for simple systems that are easy to be described by using mathematical equations. For the McKibben PAMs, this has been done in research papers such as [13]. The results show that it is rather difficult to describe the actuator in a precise way, not least because their behaviour additionally changes over time.

For this reason, the model will be generated based on the measurement data here. Each utilised PAM will therefore be tested for a defined number of pressure levels and loads. Measuring the resulting displacement will create a set of data points, which will be processed using the numerical computing tool Matlab. With the help of this software, the data points are illustrated in a 3D-plot (see Figure 5). The acquired data is interpolated, using a 5x5 polynomial fitting tool, which creates the illustrated model surface, based on an equation with 25 parameters. With the help of this model, any given pressure of the PAM can be calculated, based on the measurement of muscles load, as well as the desired displacement.

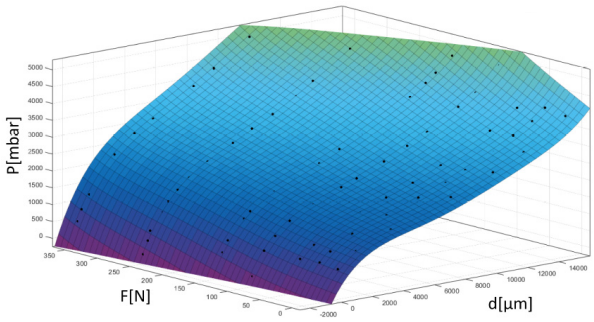

Figure 5. Measurement model of the PAM

D. Controller Design

As mentioned above, the goal of such controller is not only to get the desired trajectory, but also the required torque. Thus, a model-based controller is implemented for the PAMs, with an open loop trajectory control with force feedback and an closed-loop pressure control. The desired displacement, determined by the trajectory planning module, is used together with force feedback to get the required air pressure.

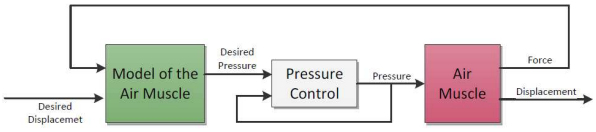

Figure 6. Block diagram of the implemented model-based controller

There are numerous ways to design a closed-loop pressure control system, while PID controller is the most commonly utilised one. In this case, the actuators have been linearized, which leads to a plant consisting of a single integrating element only. The resulting PD-controller is thus capable of operation without any steady-state error. In details, the desired pressure can be compared with the measured value, leaving an error *e*. The unsaturated controller output S_U results from:

$$S_U = K_P \cdot e + K_D \cdot \frac{de}{dt}. \tag{9}$$

Afterwards, the controller output is saturated (*S*) in order to never exceed the actuator linearization's input limits. The consequence is a linearly controlled air flow rate, which is integrated in the PAM, resulting in air pressure. This value again, is quantified by using a pressure gauge and fed back in order to calculate the error. A block diagram of the controller is illustrated in Figure 7.

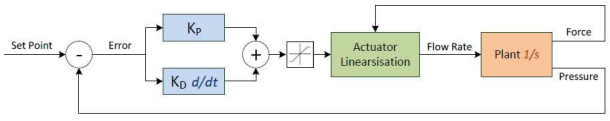

Figure 7. Block diagram of the closed-loop pressure control system

The final values for these parameters are $K_P = 2$ and $K_D = 1$, given that the control frequency is synchronised with the PWM frequency of the actuators ($f = 50$Hz).

IV. Experiment Results

The basic requirement for trajectory is to move the wrist within an arbitrary angular limit, and the safe operation of the orthosis should be incorporated. That means the trajectory planning module should monitor the force, and prevent the orthosis from taking on an angular displacement which may be unsafe for the patient's wrist. Here, the desired angle is not calculated by a predefined function, but by the integration of an adjustable speed. The maximum speed $v_{\max}$ can be set to a similar amount patients tolerate well, but it will be dampened when it approaches either the angular or the torque limit. Upon reaching one of these limits, the algebraic sign of the speed will be inverted, and the maximum speed restored. The damping of the speed *D* is calculated by the following law:

$$D = \min\left(\frac{\theta_{\max} - \theta}{k_\theta}, \frac{\tau_{\max} - \tau}{k_\tau}\right). \tag{10}$$

$$v = \begin{cases} v_{\max} \cdot D^{k_d} & D < 1 \\ v_{\max} & D \geq 1 \end{cases}. \tag{11}$$

Figure 8 illustrates the result of planned trajectory. The emerging trajectory is similar to the sine wave, if no torque is applied. The graph shows as well, that a rising torque will dampen the trajectory speed and finally result in its reversal when reaching the limit. For the validation of the closed loop pressure control, the result of this experiment is illustrated in Figure 9. The magnitude of the pressure error does not exceed 25mbar. Results of the wrist angle control, as well as the parallel force measurement, can be retrieved from Figure 10. Regarding to the angle trajectory, a small error can be observed throughout the whole sine period. In addition, the measured angle does reach the desired angle for the maximum as well as the minimum value. The mean squared error of the angle control is 6°, which is considerably low. The measured forces F_1 and F_2 have little variance, and the shape of the curves show a consistent differential force.

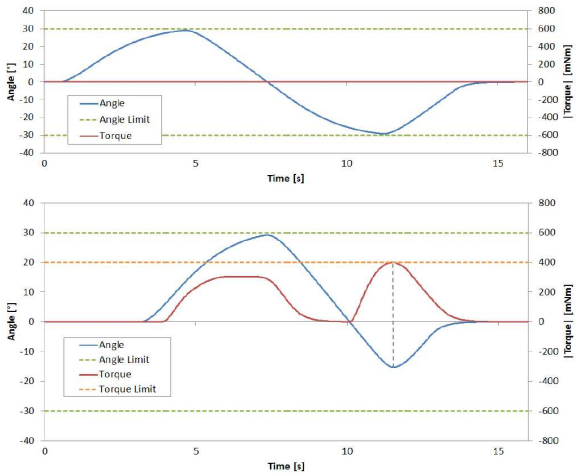

Figure 8. Safe trajectory planning: *Top*: Movement within the angular limit, no torque applied. *Bottom*: If the applied torque exceeds the predefined limit, the trajectory's speed will slow down and finally reverse.

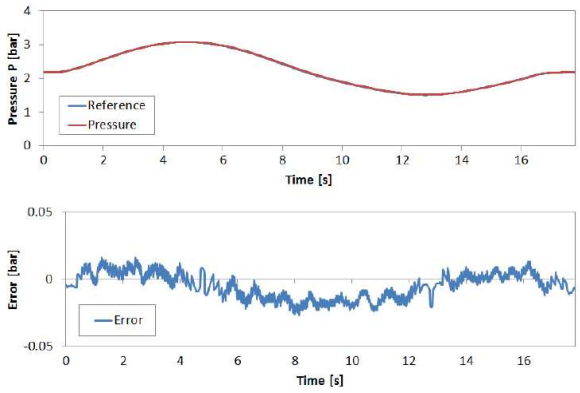

Figure 9. *Top*: Pressure curve of the presented control system. *Bottom*: Error of the curve above.

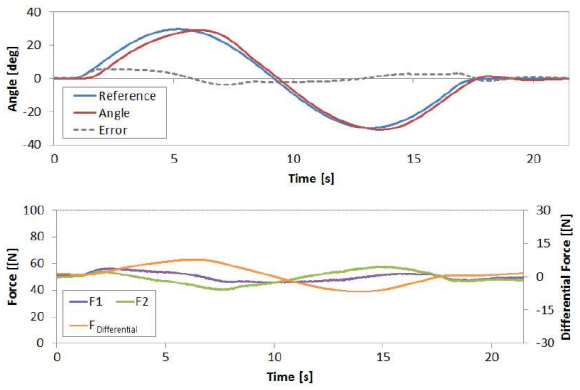

Figure 10. *Top*: Result for the open-loop angle/displacement control, including an error graph. *Bottom*: Result of the parallel force measurements.

V. Discussion and Conclusion

This paper presented the development of a robotic wrist orthosis for joint rehabilitation. Mechanical development of the orthosis and a preceding prototype was demonstrated. The primary task was to develop a control system for the utilised pneumatic actuators. As a majority of existing robots for wrist rehabilitation are applying rigid actuators, this work presents an exploratory implementation of soft wrist orthosis. To control such a PAMs-driven robot in high-performance, a model-based controller that relies on a predefined static model of the actuator was developed. The model-based controller resulted in a look-up table that characterises the relations between force and displacement parameters and the pressure within the actuator. In order to guarantee the trajectory accuracy as well the force safety, an embedded closed-loop pressure control system was implemented, in order to set the pressure in each muscle according to the desired displacement and torque. The safely trajectory planning method was used in this system to test its performance. The resulting angle curve as well as their parallel force measurements were presented. In the end, the utilised control method allowed the trajectory following with a mean squared error of 6°. The dynamic torque measurement was interfered by friction in the mechanical parts of the device, leaving the device with a measured maximum torque of about 0.1Nm during the trajectory period.

Notice that the presented PAM model is based on static behaviour of the muscle, and does not include any dynamic characteristics such as deviant behaviour for deflating and inflating the PAMs. Subsequent research on this matter shows, that a hysteresis behaviour of the PAMs has been ascertained in [12] and [19]. It is demonstrated that the tube's rubber shell does not only deform elastically, but also plastically. It means that the tube's displacement upon pressurisation is shorter than displacement for the same pressure-/force-pair upon deflation. This circumstance can only be described in a mathematical model, which assumingly requires long computation time on the real-time controller. The lack of this knowledge in the present model leads to inaccurate displacement behaviour, since the two PAMs always act in different direction (inflation/ deflation) due to the antagonistic setup.

The notable delay between measured angle and trajectory can only be introduced by the compliance of the actuators, since the actual pressure is evidently un-delayed. It is more likely that the observed differences of the muscle's behaviour are responsible for this phenomenon. Regarding the parallel force measurements, it is also obvious that the force-controlled system is able to keep both forces F_1 and F_2 at a constant level. Irrespectively of the course of the individual forces, F_D is not zero. The reason for this perhaps due to the friction occurring in several parts of the mechanical wiring system. Especially the pulleys of the hinge, which are mounted in ball bearings, are likely to cause static and dynamic friction. The redirection of the wires from the muscles towards the pulleys also induces an additional force to the system. Future work will focus on improving the trajectory and force tracking performance, and advanced robotic training methods considering human-robot interaction will be further studied.

Acknowledgment

This work is supported by the National Natural Science Foundation of China (Grant No. 51475342) and the Chinese Scholarship Council (CSC).

References

[1] H. S. Lo, S. Q. Xie, "Exoskeleton robots for upper-limb rehabilitation: State of the art and future prospects," *Medical engineering & physics,* vol. 34 no. 3, 261-268, 2012.

[2] H. I. Krebs, Hogan Neville, Aisen Mindy L., and B. Volpe, "Robot-aided neurorehabilitation," *IEEE Trans. on Rehabilitation Engineering*, vol. 6, no. 1, pp. 75–87, 1998.

[3] M. Paweł, E. Jörg, G.H. Kurt, J.T. Arne, L. Steffen, "A survey on robotic devices for upper limb rehabilitation," *Journal of Neuroengineering and Rehabilitation*, vol. 11, no. 3, 2014.

[4] W. Verna, J. Richard J., "Quantitative and qualitative analysis of joint stiffness in normal subjects and in patients with connective tissue diseases," *Ann. rheum. Dis.*, vol. 20, no. 1, pp. 36–46, 1961.

[5] H.I. Krebs, J.J. Palazzolo, L. Dipietro, M. Ferraro, J. Krol, et al., "Rehabilitation robotics: Performance-based progressive robot-assisted therapy," *Autonomous Robots*, vol. 15, no. 1, pp. 7–20, 2003.

[6] J.A. Rogers, "A clear advance in soft actuators," *Science*, vol. 341, no. 6149, pp. 968–969, 2013.

[7] K. Kiguchi, K. Iwami, M. Yasuda, K. Watanabe, and T. Fukuda, "An exoskeletal robot for human shoulder joint motion assist," *IEEE/ASME Trans. on Mechatronics*, vol. 8, no. 1, pp. 125–135, 2003.

[8] A. Mirelman, P. Bonato, J.E. Deutsch, "Effects of training with a robot-virtual reality system compared with a robot alone on the gait of individuals after stroke," *Stroke*, vol. 40, no. 1, pp. 169–174, 2009.

[9] E. J. Lenze, M. C. Munin, T. Quear, M. A. Dew, J. C. Rogers, A. E. Begley, et al,, "Significance of poor patient participation in physical and occupational therapy for functional outcome and length of stay," *Archives of Physical Medicine and Rehabilitation*, vol. 85, no. 10, pp. 1599–1601, 2004.

[10] B. Rohrer, S. Fasoli, H. I. Krebs, R. Hughes, B. Volpe, W. R. Frontera, et al., "Movement smoothness changes during stroke recovery," *The Journal of Neuroscience*, vol. 22, no. 18, pp. 8297–8304, 2002.

[11] P. K., Jamwal, S. Q. Xie, S. Hussain and J. G. Parsons. "An adaptive wearable parallel robot for the treatment of ankle injuries*." IEEE/ASME Transactions on Mechatronics*, vol. 19, no. 1, 64-75, 2014.

[12] C.P. Chou, B. Hannaford, "Measurement and modeling of mckibben pneumatic artificial muscles," *IEEE Trans. On Robot*, vol. 12, no. 1, pp. 90–102, 1996.

[13] B. Tondu and P. Lopez, "Modeling and control of mckibben artificial muscle robot actuators," *IEEE Control Systems*, vol. 20, no. 2, pp. 15–38, 2000.

[14] ˇSitum ˇ Z., Herceg S., Ed., *Design and Control of a Manipulator Arm Driven by Pneumatic Muscle Actuators*, 2008.

[15] S. Hussain, S. Q. Xie, P. K. Jamwal, "Adaptive impedance control of a robotic orthosis for gait rehabilitation," *IEEE Transactions on Cybernetics*, vol. 43, no.3, 1025-1034, 2013.

[16] S. Q. Xie, P. K. Jamwal, "An iterative fuzzy controller for pneumatic muscle driven rehabilitation robot," *Expert Systems with Applications* vol. 38, no.7, 8128-8137, 2011.

[17] "Fluidic muscle dmsp/mas," April 2013.

[18] Festo AG, "Festo fluidic muscle," 04.11.2014. [Online]. Available: http://www.festo. com/cms/en_corp/9790.htm

[19] M. Damme, P. Beyl, B. Vanderborght, R. van Ham, I. Vanderniepen, R. Versluys, et al., "Modeling hysteresis in pleated pneumatic artificial muscles: robotics", *IEEE Conf. on Automation and Mechatronics*, 2008.